13. J. S. Dasen, A. De Camilli, B. Wang, P. W. Tucker, T. M. Jessell, *Cell* **134**, 304–316 (2008).
14. J. R. Keast, *Int. Rev. Cytol.* **248**, 141–208 (2006).
15. J. R. Keast, *Neuroscience* **66**, 655–662 (1995).
16. A. Kuntz, R. L. Moseley, *J. Comp. Neurol.* **64**, 63–75 (1936).
17. W. C. De Groat, A. M. Booth, J. Krier, in *Integrative Functions of the Autonomic Nervous System*, C. M. Brooks, K. Koizumi, A. Sato, Eds. (University of Tokyo Press, Tokyo, 1979), pp. 234–245.
18. U. Ernsberger, H. Rohrer, *Cell Tissue Res.* **297**, 339–361 (1999).
19. K. Huber *et al.*, *Dev. Biol.* **380**, 286–298 (2013).
20. K. Tsarovina *et al.*, *Development* **131**, 4775–4786 (2004).
21. E. Doxakis, L. Howard, H. Rohrer, A. M. Davies, *EMBO Rep.* **9**, 1041–1047 (2008).
22. L. Huber, M. Ferdin, J. Holzmann, J. Stubbusch, H. Rohrer, *Dev. Biol.* **363**, 219–233 (2012).
23. C. L. Yntema, W. S. Hammond, *J. Exp. Zool.* **129**, 375–413 (1955).
24. V. Dyachuk *et al.*, *Science* **345**, 82–87 (2014).
25. I. Espinosa-Medina *et al.*, *Science* **345**, 87–90 (2014).
26. S. Nilsson, in *Autonomic Nerve Function in the Vertebrates*, *Zoophysiology*, vol. 13, D. S. Farner, Ed. (Springer-Verlag, New York, 1983), chap. 2.
27. C. Olsson *et al.*, *J. Comp. Neurol.* **496**, 787–801 (2006).
28. K. Fukai, H. Fukuda, *J. Physiol.* **362**, 69–78 (1985).
29. W. Jänig, *The Integrative Action of the Autonomic Nervous System: Neurobiology of Homeostatis* (Cambridge Univ. Press, Cambridge, UK, 2006).
30. W. C. de Groat, W. R. Saum, *J. Physiol.* **220**, 297–314 (1972).
31. A. Pattyn, X. Morin, H. Cremer, C. Goridis, J. F. Brunet, *Nature* **399**, 366–370 (1999).

**ACKNOWLEDGMENTS**

We thank the Imaging Facility of Institut de Biologie de l'École Normale Supérieure (IBENS), which is supported by grants from Fédération pour la Recherche sur le Cerveau, Région Ile-de-France DIM NeRF 2009 and 2011 and France-BioImaging. We thank A. Shihavuddin and A. Genovesio for help with image analysis, the animal facility of IBENS, C. Goridis for helpful comments on the manuscript, and all the members of the Brunet laboratory for discussions. This study was supported by the Centre National de la Recherche Scientifique, the Ecole Normale Supérieure, Institut National de la Santé et de la Recherche Médicale, Agence Nationale de la Recherche (ANR) award ANR-12-BSV4-0007-01 (to J.-F.B), Fondation pour la Recherche Médicale (FRM) award DEq. 2000326472 (to J.-F.B.), the Investissements d'Avenir program of the French government implemented by the ANR (referenced ANR-10-LABX-54 MEMO LIFE and ANR-11-IDEX-0001-02 Paris Sciences et Lettres Research University). I.E.-M. was supported by the French Ministry of Higher Education and Research and the FRM award FDT20160435297. Work in W.D.R.'s laboratory is supported by the European Research Council (grant agreement 293544) and Wellcome (100269/Z/12/Z). The supplementary materials contain additional data.

**SUPPLEMENTARY MATERIALS**

www.sciencemag.org/content/354/6314/893/suppl/DC1
Materials and Methods
Figs. S1 to S11
Movies S1 and S2
References (*32*–*43*)

12 July 2016; accepted 14 October 2016
10.1126/science.aah5454

PLANT SCIENCE

# Phytochrome B integrates light and temperature signals in *Arabidopsis*

**Martina Legris,[1] Cornelia Klose,[2]* E. Sethe Burgie,[3]* Cecilia Costigliolo Rojas,[1]* Maximiliano Neme,[1] Andreas Hiltbrunner,[2,4] Philip A. Wigge,[5] Eberhard Schäfer,[2,4]† Richard D. Vierstra,[3]† Jorge J. Casal[1,6]‡**

**Ambient temperature regulates many aspects of plant growth and development, but its sensors are unknown. Here, we demonstrate that the phytochrome B (phyB) photoreceptor participates in temperature perception through its temperature-dependent reversion from the active Pfr state to the inactive Pr state. Increased rates of thermal reversion upon exposing *Arabidopsis* seedlings to warm environments reduce both the abundance of the biologically active Pfr-Pfr dimer pool of phyB and the size of the associated nuclear bodies, even in daylight. Mathematical analysis of stem growth for seedlings expressing wild-type phyB or thermally stable variants under various combinations of light and temperature revealed that phyB is physiologically responsive to both signals. We therefore propose that in addition to its photoreceptor functions, phyB is a temperature sensor in plants.**

Plants have the capacity to adjust their growth and development in response to light and temperature cues (*1*). Temperature-sensing helps plants determine when to germinate, adjust their body plan to protect themselves from adverse temperatures, and flower. Warm temperatures as well as reduced light resulting from vegetative shade promote stem growth, enabling seedlings to avoid heat stress and canopy shade from neighboring plants. Whereas light perception is driven by a collection of identified photoreceptors—including the red/far-red light-absorbing phytochromes; the blue/ultraviolet-A (UV-A) light–absorbing cryptochromes, phototropins, and members of the Zeitlupe family; and the UV-B–absorbing UVR8 (*2*)—temperature sensors remain to be established (*3*). Finding the identity (or identities) of temperature sensors would be of particular relevance in the context of climate change (*4*).

Phytochrome B (phyB) is the main photoreceptor controlling growth in *Arabidopsis* seedlings exposed to different shade conditions (*5*). Like others in the phytochrome family, phyB is a homodimeric chromoprotein, with each subunit harboring a covalently bound phytochromobilin chromophore. phyB exists in two photo-interconvertible forms: a red light–absorbing Pr state that is biologically inactive and a far-red light–absorbing Pfr state that is biologically active (*6*, *7*). Whereas Pr arises upon assembly with the bilin, formation of Pfr requires light, and its levels are strongly influenced by the red/far-red light ratio. Consequently, because red light is absorbed by photosynthetic pigments, shade light from neighboring vegetation has a strong impact on Pfr levels by reducing this ratio (*8*). phyB Pfr also spontaneously reverts back to Pr in a light-independent reaction called thermal reversion (*9*–*11*). Traditionally, thermal reversion was assumed to be too slow relative to the light reactions to affect the Pfr status of phyB, even under moderate irradiances found in natural environments, but two observations contradict this view. First, the formation of phyB nuclear bodies, which reflects the status of Pfr, is affected by light up to irradiances much higher than expected if thermal reversion were slow (*12*). Second, it is now clear that thermal reversion occurs in two steps. Although the first step, from the Pfr:Pfr homodimer (D2) to the Pfr:Pr heterodimer (D1), is slow ($k_{r2}$), the second step, from the Pfr:Pr heterodimer to the Pr:Pr homodimer (D0), is almost two orders of magnitude faster ($k_{r1}$) (Fig. 1A) (*11*).

Physiologically relevant temperatures could change the magnitude of $k_{r1}$ and consequently affect Pfr and D2 levels, even under illumination (Fig. 1A). To test this hypothesis, we used in vitro and in vivo spectroscopy and analysis of phyB nuclear bodies by means of confocal microscopy. For the first of these approaches, we produced recombinant full-length phyB bearing its phytochromobilin chromophore. When irradiated under continuous red light, the in vitro absorbance at 725 nm reached lower values at higher temperatures, which is indicative of reduced steady-state levels of Pfr (Fig. 1, B and C). We calculated the differences between the steady-state absorbance spectra in darkness and continuous red light (Δ absorbance). The amplitude between the maximum and minimum peaks of Δ absorbance, which represents the amount of Pfr, strongly decreased between 10 and 30°C (Fig. 1, D and E). This characteristic of phyB differs from the typical behavior

[1]Fundación Instituto Leloir, Instituto de Investigaciones Bioquímicas de Buenos Aires–Consejo Nacional de Investigaciones Científicas y Técnicas (CONICET), 1405 Buenos Aires, Argentina. [2]Institut für Biologie II, University of Freiburg, Schaenzlestrasse 1, D-79104 Freiburg. [3]Department of Biology, Washington University in St. Louis, Campus Box 1137, One Brookings Drive, St. Louis, MO 63130, USA. [4]BIOSS Centre for Biological Signaling Studies, University of Freiburg, Schaenzlestrasse 18, 79104 Freiburg, Germany. [5]Sainsbury Laboratory, Cambridge University, 47 Bateman Street, Cambridge CB2 1LR, UK. [6]Instituto de Investigaciones Fisiológicas y Ecológicas Vinculadas a la Agricultura (IFEVA), Facultad de Agronomía, Universidad de Buenos Aires and CONICET, Avenida San Martín 4453, 1417 Buenos Aires, Argentina.
*These authors contributed equally to this work. †These authors contributed equally to this work. ‡**Corresponding author. Email: casal@ifeva.edu.ar**

Corrected 17 November 2016. See full text.

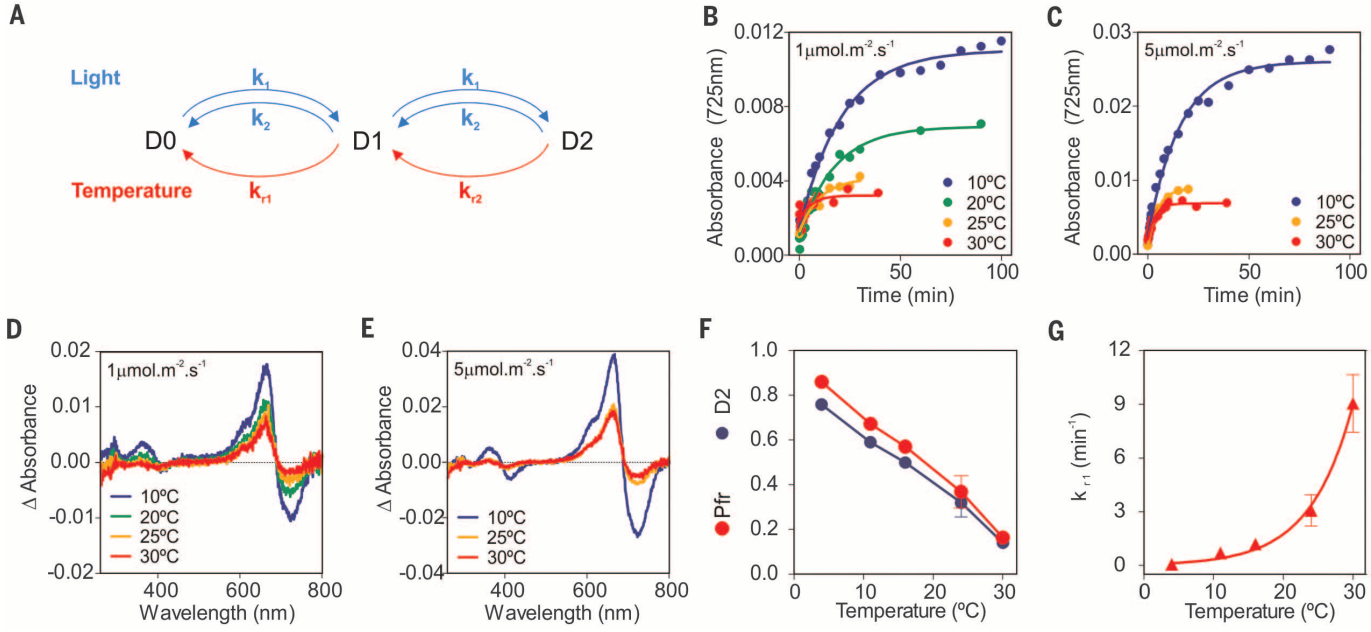


**Fig. 1. The status of phyB responds to light and temperature.** (**A**) Three-stage model of phyB (*11*). Our working hypothesis is that D2 integrates light cues (via $k_1$ and $k_2$) and temperature cues (via $k_{r2}$ and mainly $k_{r1}$). (**B** to **E**) Warm temperatures reduce Pfr levels of full-length recombinant phyB exposed in vitro to 1 [(B) and (D)] or 5.1 [(C) and (E)] µmol $m^{-2}$ $s^{-1}$ of continuous red light. [(B) and (C)] Absorbance kinetics (maximal absorption decreased with temperature, $P < 0.05$). [(D) and (E)] Δ absorbance in samples incubated in darkness or exposed to continuous red light to reach a steady state. The difference between Δ absorbance at 665 and 725 nm decreased with temperature ($P < 0.01$). (**F**) Warm temperatures reduce the levels of Pfr and D2 in vivo measured in *phyA* mutant seedlings overexpressing phyB (*9*) exposed to 1 µmol $m^{-2}$ $s^{-1}$ red light. Means ± SE of three biological replicates. (**G**) Warm temperatures increase $k_{r1}$ [calculated from (F), $P < 0.001$].

of enzymes, which exhibit increased activity over the same temperature range (*13*).

We also measured with in vivo spectroscopy the steady-state levels of phyB Pfr in seedlings irradiated with continuous red or white light at different temperatures (applied only during the irradiation). Increasing temperatures reduced both the total pool of Pfr and that of D2 (Fig. 1F and fig. S1), which is considered to be the physiologically relevant species for phyB (*11*). Using these data, we determined $k_{r1}$, which increased with temperature (Fig. 1G).

phyB nuclear body formation increases with irradiance and red/far-red light ratio (*12*, *14*) because it depends on D2 (*11*). As a proxy for temperature impact on D2, we used the difference in nuclear body formation in lines of the *phyB-9*–null mutant rescued with unmodified phyB [phyB–yellow fluorescent protein (YFP)] or either of two chromophore pocket mutants that suppress Pfr thermal reversion in vitro with little to no effect on photoconversion ($phyB^{Y361F}$-YFP and $phyB^{R582A}$-YFP) (*15*, *16*). De-etiolated (green) seedlings were transferred to the different light conditions (irradiances and red/far-red light ratios) representative of unfiltered sunlight, canopy shade, or cloudy days, in combination with different temperatures applied only during the light treatments (fig. S2). The nuclear body size of $phyB^{Y361F}$-YFP and $phyB^{R582A}$-YFP was not significantly affected by irradiance (fig. S3) and strongly affected by the red/far-red ratio (fig. S4). This is consistent with the notion that irradiance responses depend on $k_{r1}$ and $k_{r2}$ (*11*), which are affected in the mutants. The size of phyB nuclear bodies varied quadratically with temperature and

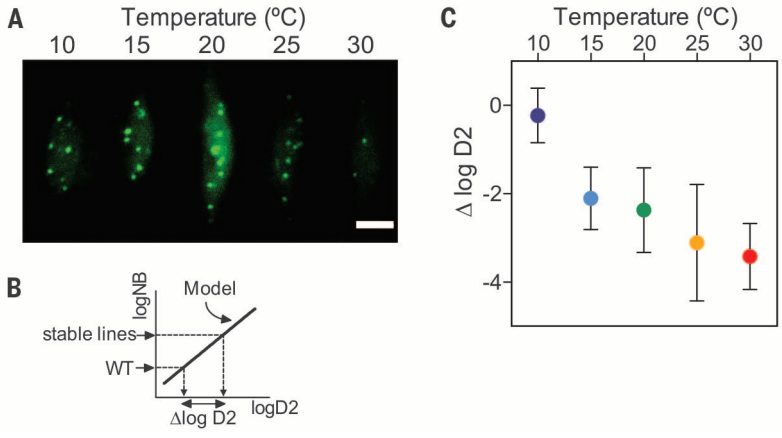


**Fig. 2. phyB nuclear bodies respond to light and temperature.** (**A**) Dual response of phyB-YFP nuclear bodies to temperature (white light, 10 µmol $m^{-2}$ $s^{-1}$). Scale bar, 5 µm. (**B**) Estimation of D2 in the wild type by using its average phyB nuclear body size (NB) as input in the model relating NB to D2 in lines expressing stabilized phyB ($phyB^{Y361F}$-YFP and $phyB^{R582A}$-YFP). (**C**) Impact of temperature on D2. Difference in log-transformed D2 averaged for 5 to 11 conditions (±SE) covering a wide range of irradiances and red/far-red ratios (temperature effect, $P < 0.05$).

was largest at ~20°C (Fig. 2A and fig. S5). We tested the hypothesis that the negative phase of this response to temperature is the manifestation of enhanced thermal reversion reducing D2. Toward this aim, we modeled the average size of the $phyB^{Y361F}$-YFP and $phyB^{R582A}$-YFP nuclear bodies (tables S1 and S2) as a function of both D2 (*11*) and temperature effects not mediated by changes in D2 (fig. S6). Then, we used this restricted model to predict D2 levels from phyB nuclear body sizes in wild-type lines (Fig. 2B). The difference between the apparent log D2 in wild-type and the log D2 of $phyB^{Y361F}$ and $phyB^{R582A}$ in the same light condition is shown in Fig. 2C (difference averaged for all light conditions). The results indicate that high temperatures decrease the apparent D2 for the wild-type phyB under a wide range of light conditions.

By using the three approaches above, we showed that the activity of phyB decreases with increasing temperature (Figs. 1 and 2), suggesting two possible biological outcomes. One is that downstream

Corrected 17 November 2016. See full text.



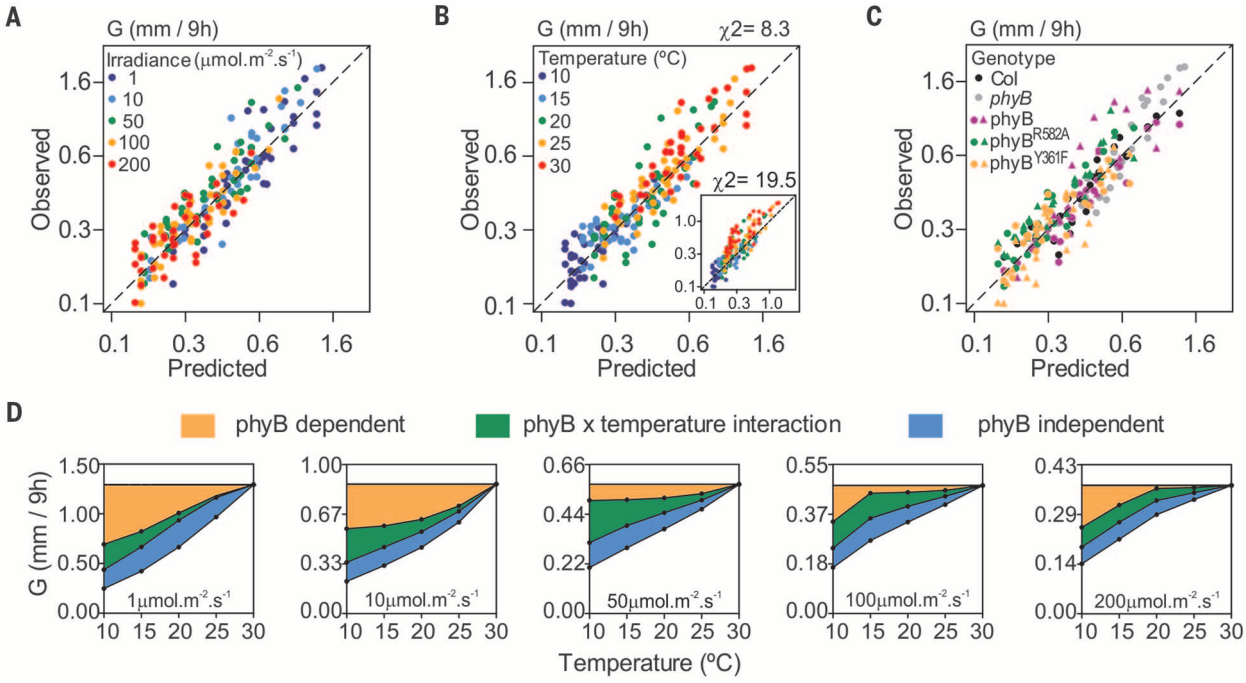


**Fig. 3. phyB mediates growth responses to light and temperature.** (**A** to **C**) Observed values of hypocotyl growth (*G*) in white light–grown seedlings of eight genotypes exposed to 25 combinations of irradiance and temperature versus the values predicted by the growth model. The different irradiances (A), temperatures (B), and genotypes (C) are color-coded to show that the relationship between observed and predicted values is not biased for any of these factors (within the range tested here). Col, Columbia wild type; *phyB*, phyB null mutant; phyB, $phyB^{Y361F}$, and $phyB^{R582A}$, transgenic lines expressing wild-type or mutated phyB in the *phyB* null mutant background. [(B), inset] The goodness of fit of the model (Pearson's $\chi^2$ test) is greatly deteriorated when temperature effects on D2 are not incorporated (both versions of the model have the same number of parameters). (**D**) Contribution to the inhibition of growth of each one of the three temperature-dependent terms of the growth model. Topmost line is the horizontal base line of no low-temperature effects (*G* incorporating only light effects at 30°C). Downward, the lines indicate *G* calculations successively incorporating the phyB-dependent temperature effects, the phyB-temperature interaction, and the phyB-independent temperature effect. The colored areas highlight the contribution of each additional term incorporated in the calculations.

changes in phyB signaling compensate for the temperature effect. The circadian clock provides an example of temperature compensation (*17*). The other is that phyB perception of temperature cues controls the physiological output. A prediction of the latter hypothesis is that phyB activity (D2) should similarly affect growth independently of whether it is altered by light, temperature, or mutations that stabilize phyB. To test this prediction, we cultivated *Arabidopsis* seedlings (including phyB genetic variants) at the same irradiance and temperature, sorted them to the different light and temperature environments (fig. S2), and modeled growth under these conditions (table S3) as a function of D2.

The growth responses to temperature (fig. S7) and light (*18*) are not exclusively mediated by phyB (D2). Thus, we built the model in two steps: first, fitting univariate submodels describing the relationship between growth and the individual factors (D2, temperature effects not mediated by changes in D2, and activity of other photo-sensory receptors), and then combining those components in the final model. To quantify the contribution of D2 (fig. S8), we used growth at 30°C (no low-temperature inhibition of growth) (fig. S9) of all genotypes, including the stabilized phyB variants and the *phyB*-null mutant (D2 = 0). To quantify the effects of temperature not mediated by changes in D2 (fig. S9B), we used the *phyB* mutant (no phyB-mediated inhibition) at 1 µmol $m^{-2}$ $s^{-1}$ (at this irradiance, and at 30°C, growth is maximal, indicating that other photoreceptors do not make a strong contribution). To quantify the contribution of other photoreceptors (fig. S10), we used the *phyB* mutant (no phyB-mediated inhibition) at a range of irradiances at 30°C (no low-temperature growth inhibition). The only statistically significant interaction among these terms was between D2 and temperature effects not mediated by changes in D2 (table S4). Therefore, in the final model, growth was inversely related to terms representing the actions of D2, low temperatures (not mediated by changes in D2), other photo-sensory receptors, and the synergistic interaction between D2 and low temperature (not mediated by changes in D2).

We then fitted to the model growth for all 200 light-temperature-genotype combinations. The relationship between observed and predicted data showed no systematic deviation from the 1:1 correlation for the different light (Fig. 3A), temperature (Fig. 3B), or genetic variants with altered Pfr stability (Fig. 3C). Predicted data were obtained with D2 values affected by light, temperature, and genotype. To test the significance of temperature effects mediated by changes in the status of phyB, we recalculated growth by using D2 modified by light and genotype but not by temperature (constant 10°C). This adjustment reduced the growth model goodness of fit (Fig. 3B, inset), indicating that the contribution of phyB-mediated temperature effects on growth is statistically significant and should not be neglected. Because we estimated the effect of D2 using data from a single temperature (fig. S8), our growth model is not based on the assumption that D2 changes with temperature, thus providing confidence that the latter conclusion is genuine.

We used the growth model to compare the contribution of each of the three temperature-dependent terms to the inhibition of growth by low temperatures. phyB-mediated effects of temperature contribute to the overall temperature response (Fig. 3D). The effects were large at low irradiances, decreased with intermediate irradiances (light reactions become increasingly important), and increased again at higher irradiances because now D2 affects growth more strongly.

Phytochromes were discovered and have been studied on the basis of their roles as light receptors in plants (*6*, *7*). However, our observations that temperature alters the amount of D2 for phyB (Figs. 1 and 2) and its physiological output in a manner similar to light (Fig. 3) indicate that phyB should also be defined as a temperature cue receptor. phyB requires light to comply with this temperature function by needing light to initially generate the unstable but bioactive Pfr state. Temperature affects the Pfr status of phyB mainly via $k_{r1}$ in the light (Fig. 1) and via $k_{r2}$ during the night (*19*). Receptors are often activated by their

Corrected 17 November 2016. See full text.

ligands; although phyB is activated by red light, it is inactivated by far-red light and high temperatures. This combination of light and temperature perception would serve to integrate the signals controlling photo- and thermo-morphogenesis in ways that optimize the growth of plants exposed to a wide range of environments.

## REFERENCES AND NOTES


1. J. J. Casal, C. Fankhauser, G. Coupland, M. A. Blázquez, *Trends Plant Sci.* **9**, 309–314 (2004).
2. V. C. Galvão, C. Fankhauser, *Curr. Opin. Neurobiol.* **34**, 46–53 (2015).
3. M. Quint *et al.*, *Nat. Plants* **2**, 15190 (2016).
4. D. S. Battisti, R. L. Naylor, *Science* **323**, 240–244 (2009).
5. J. J. Casal, *Annu. Rev. Plant Biol.* **64**, 403–427 (2013).
6. P. H. Quail *et al.*, *Science* **268**, 675–680 (1995).
7. E. S. Burgie, R. D. Vierstra, *Plant Cell* **26**, 4568–4583 (2014).
8. M. G. Holmes, H. Smith, *Photochem. Photobiol.* **25**, 539–545 (1977).
9. U. Sweere *et al.*, *Science* **294**, 1108–1111 (2001).
10. É. Ádám *et al.*, *PLOS ONE* **6**, e27250 (2011).
11. C. Klose *et al.*, *Nat. Plants* **1**, 15090 (2015).
12. S. A. Trupkin, M. Legris, A. S. Buchovsky, M. B. Tolava Rivero, J. J. Casal, *Plant Physiol.* **165**, 1698–1708 (2014).
13. M. E. Salvucci, K. W. Osteryoung, S. J. Crafts-Brandner, E. Vierling, *Plant Physiol.* **127**, 1053–1064 (2001).
14. E. K. Van Buskirk, P. V. Decker, M. Chen, *Plant Physiol.* **158**, 52–60 (2012).
15. J. Zhang, R. J. Stankey, R. D. Vierstra, *Plant Physiol.* **161**, 1445–1457 (2013).
16. E. S. Burgie, A. N. Bussell, J. M. Walker, K. Dubiel, R. D. Vierstra, *Proc. Natl. Acad. Sci. U.S.A.* **111**, 10179–10184 (2014).
17. P. A. Salomé, D. Weigel, C. R. McClung, *Plant Cell* **22**, 3650–3661 (2010).
18. R. Sellaro *et al.*, *Plant Physiol.* **154**, 401–409 (2010).
19. J.-H. Jung *et al.*, *Science* **354**, 886–889 (2016).


## ACKNOWLEDGMENTS

We thank F. Venezia (University of Freiburg) for his valuable help with the analytical equations. This work was supported by Agencia Nacional de Promoción Científica y Tecnológica (grants PICT 2012-1396 and PICT 2013-1444 to J.J.C.), Alexander von Humboldt-Foundation (J.J.C.), Universidad de Buenos Aires (grant 20020100100437 to J.J.C.), Fundación Rene Baron (J.J.C.), the Excellence Initiative of the German Federal and State Governments (EXC 294, project C 20 to E.S. and A.H.), the German Research Foundation (DFG; SCHA 303/16-1 and HI 1369/5-1 to E.S. and A.H.), and the U.S. National Science Foundation (MCB-1329956 to R.D.V.). R.D.V and E.S.B. and the University of Wisconsin–Madison have filed U.S. patent application P140220US02, which relates to the use of mutants phyB$^{Y361F}$ and phyB$^{R582A}$ in agriculture. The supplementary materials contain additional data.

## SUPPLEMENTARY MATERIALS

www.sciencemag.org/content/354/6314/897/suppl/DC1
Materials and Methods
Figs. S1 to S11
Tables S1 to S4
References (*20*–*26*)

9 March 2016; accepted 16 September 2016
Published online 27 October 2016
10.1126/science.aaf5656

SYNTHETIC BIOLOGY

# A synthetic pathway for the fixation of carbon dioxide in vitro

**Thomas Schwander,[1] Lennart Schada von Borzyskowski,[1,2] Simon Burgener,[1,2] Niña Socorro Cortina,[1] Tobias J. Erb[1,2,3]***

**Carbon dioxide ($CO_2$) is an important carbon feedstock for a future green economy. This requires the development of efficient strategies for its conversion into multicarbon compounds. We describe a synthetic cycle for the continuous fixation of $CO_2$ in vitro. The crotonyl–coenzyme A (CoA)/ethylmalonyl-CoA/hydroxybutyryl-CoA (CETCH) cycle is a reaction network of 17 enzymes that converts $CO_2$ into organic molecules at a rate of 5 nanomoles of $CO_2$ per minute per milligram of protein. The CETCH cycle was drafted by metabolic retrosynthesis, established with enzymes originating from nine different organisms of all three domains of life, and optimized in several rounds by enzyme engineering and metabolic proofreading. The CETCH cycle adds a seventh, synthetic alternative to the six naturally evolved $CO_2$ fixation pathways, thereby opening the way for in vitro and in vivo applications.**

Autotrophic carbon fixation transforms more than 350 gigatons of $CO_2$ annually. More than 90% of the carbon is fixed by the Calvin-Benson-Bassham (CBB) cycle in plants, algae, and microorganisms. The rest is converted through alternative autotrophic $CO_2$ fixation pathways (*1*, *2*). Despite this naturally existing diversity, the application of $CO_2$-fixing enzymes and pathways for converting $CO_2$ into value-added multicarbon products has been limited in chemistry (*3*, *4*) and biotechnology (*5*). Natural $CO_2$ fixation delivers mainly biomass and not a dedicated product. Moreover, under optimal conditions, biological $CO_2$ fixation is often directly affected by the inefficiency of the $CO_2$-fixing enzymes and pathways. For instance, the CBB cycle's carboxylase, RuBisCO (ribulose-1,5-bisphosphate carboxylase/oxygenase), is a slow catalyst that shows a strong side reaction with oxygen, which leads to the loss of fixed carbon and thus photosynthetic energy by up to 30% in a process called photorespiration (*6*).

Attempts to improve biological $CO_2$ fixation (*7*) have included evolving RuBisCO toward higher reaction rate and specificity (*8*, *9*), engineering more efficient photorespiration (*10*, *11*), and transplanting natural $CO_2$ fixation pathways into non-autotrophic organisms such as *Escherichia coli* (*12*–*14*). In contrast to these efforts, which showed only limited success, the emerging field of synthetic biology provides an alternative approach to create designer $CO_2$ fixation pathways. By freely combining different enzymatic reactions from various biological sources, completely artificial $CO_2$ fixation routes may be constructed that are kinetically or thermodynamically favored relative to the naturally evolved $CO_2$ fixation pathways. Several synthetic routes for $CO_2$ fixation have been theoretically considered (*15*). However, the gap between theoretical design and experimental realization in synthetic biology has impeded the realization of such artificial pathways. For example, attempts to directly assemble synthetic pathways in living organisms are challenged by limited understanding of the complex interplay among the different enzymes used in these synthetic networks, as well as interference of the synthetic networks in the complex background of the host organism, which can lead to undesired effects such as side reactions and toxicity. Therefore, the realization of synthetic pathways requires novel strategies that first allow their testing and optimization in more defined conditions (*16*–*19*). To overcome these limitations, we decided to take a radically different, reductionist approach by assembling a synthetic $CO_2$ fixation cycle from its principal components in a bottom-up fashion (fig. S1).

A known bottleneck in natural $CO_2$ fixation is the efficiency of a carboxylating enzyme in a given pathway (*20*–*22*). To identify a suitable $CO_2$ fixation reaction for our synthetic cycle, we first compared the different biochemical and kinetic properties of all known major carboxylase classes (*23*) (table S1). On the basis of this analysis, we decided to rely on coenzyme A (CoA)–dependent carboxylases, and enoyl-CoA carboxylases/reductases (ECRs) in particular, because of their favorable catalytic properties. ECRs are a recently discovered class of carboxylases that operate in secondary metabolism, as well as in central carbon metabolism of α-proteobacteria and *Streptomycetes*, but notably not in any autotrophic $CO_2$ fixation pathway known so far (*24*). Relative to other carboxylases, including RuBisCO, ECRs span a broad substrate spectrum (*25*), are oxygen-insensitive, do not accept molecular oxygen as substrate, require only the ubiquitous redox cofactor NADPH (reduced nicotinamide adenine dinucleotide phosphate), and catalyze the fixation of $CO_2$ with high catalytic efficiency (i.e., on average better than RuBisCO by a factor of 2 to 4) (table S1) (*26*).

We conceived several theoretical $CO_2$ fixation routes that (i) start with a given ECR reaction, (ii) regenerate the carboxylation substrate to allow for continuous cycling, and (iii) feature a dedicated output reaction to channel the fixed carbon into a product (fig. S2). In contrast to earlier approaches (*15*, *27*), we did not restrict our design to known

[1]Biochemistry and Synthetic Biology of Microbial Metabolism Group, Max Planck Institute for Terrestrial Microbiology Marburg, D-35043 Marburg, Germany. [2]Institute for Microbiology, ETH Zürich, CH-8093 Zürich, Switzerland. [3]LOEWE Center for Synthetic Microbiology, Universität Marburg, D-35037 Marburg, Germany.
*Corresponding author. Email: toerb@mpi-marburg.mpg.de

Science
AAAS

**Phytochrome B integrates light and temperature signals in *Arabidopsis***

Martina Legris, Cornelia Klose, E. Sethe Burgie, Cecilia Costigliolo Rojas Rojas, Maximiliano Neme, Andreas Hiltbrunner, Philip A. Wigge, Eberhard Schäfer, Richard D. Vierstra and Jorge J. Casal

(October 27, 2016)
*Science* **354** (6314), 897-900. [doi: 10.1126/science.aaf5656]
originally published online October 27, 2016

Editor's Summary

**Combining heat and light responses**

Plants integrate a variety of environmental signals to regulate growth patterns. Legris *et al.* and Jung *et al.* analyzed how the quality of light is interpreted through ambient temperature to regulate transcription and growth (see the Perspective by Halliday and Davis). The phytochromes responsible for reading the ratio of red to far-red light were also responsive to the small shifts in temperature that occur when dusk falls or when shade from neighboring plants cools the soil.

*Science*, this issue p. 897, p. 886; see also p. 832



*Science* (print ISSN 0036-8075; online ISSN 1095-9203) is published weekly, except the last week in December, by the American Association for the Advancement of Science, 1200 New York Avenue NW, Washington, DC 20005. 